American Industrial Hygiene Association Journal

ISSN: 0002-8894 (Print) (Online) Journal homepage: https://www.tandfonline.com/loi/aiha20

Nonuniform Air Flow in Inlets: the Effect on Filter Deposits in the Fiber Sampling Cassette

Paul A. Baron , Chih-Chieh Chen , David R. Hemenway & Patrick O'Shaughnessy

To cite this article: Paul A. Baron , Chih-Chieh Chen , David R. Hemenway & Patrick O'Shaughnessy (1994) Nonuniform Air Flow in Inlets: the Effect on Filter Deposits in the Fiber Sampling Cassette, American Industrial Hygiene Association Journal, 55:8, 722-732, DOI: 10.1080/15428119491018619

To link to this article: https://doi.org/10.1080/15428119491018619

Published online: 04 Jun 2010.

NONUNIFORM AIR FLOW IN INLETS: THE EFFECT ON FILTER DEPOSITS IN THE FIBER SAMPLING CASSETTE

Paul A. Baron[a]
Chih-Chieh Chen[a]
David R. Hemenway[b]
Patrick O'Shaughnessy[b]

[a]Division of Physical Sciences and Engineering, National Institute for Occupational Safety and Health, Centers for Disease Control and Prevention, Public Health Service, Department of Health and Human Services, 4676 Columbia Parkway, Cincinnati, OH 45226; [b]The University of Vermont, College of Engineering and Mathematics, Votey Building, Burlington, VT 05405-3800

Smoke stream studies were combined with a new technique for visualizing a filter deposit from samples used to monitor asbestos or other fibers. Results clearly show the effect of secondary flow vortices within the sampler under anisoaxial sampling conditions. The vortices observed at low wind velocities occur when the inlet axis is situated at angles between 45° and 180° to the motion of the surrounding air. It is demonstrated that the vortices can create a complex nonuniform pattern in the filter deposit, especially when combined with particle settling or electrostatic interactions between the particles and the sampler. Inertial effects also may play a role in the deposit nonuniformity, as well as causing deposition on the cowl surfaces. Changes in the sampler, such as its placement, may reduce these biases. The effects noted are not likely to occur in all sampling situations, but may explain some reports of high variability on asbestos fiber filter samples. The flow patterns observed in this study are applicable to straight, thin-walled inlets. Although only compact particles were used, the air flow patterns and forces involved will have similar effects on fibers of the same aerodynamic diameter.

An important requirement for aerosol samples taken in the workplace and in other environments is that the sample be representative of the aerosol present in that environment. Thus, aerosol must enter the sampler and be deposited on the collection medium (usually a filter) without loss or modification. Some measurement techniques further require that the sample be uniformly deposited on the filter. For example, asbestos fiber analytical methods require such uniform deposition because only small, randomly chosen locations on the filter are observed in the analysis. Sampling for asbestos and other fibers is currently conducted with a 25-mm diameter filter cassette, with a 50-mm long straight tubular inlet called a cowl.[1]

Mention of product or company name does not constitute endorsement by the Centers for Disease Control and Prevention.

To understand aerosol sampling, a good understanding of the air flow surrounding and within the sampler is required. The most easily characterized sampler uses isokinetic, isoaxial flow conditions at the inlet. However, this is not possible under most workplace situations, especially when the sampler is being worn by a worker. It is sometimes assumed that the air flow entering and passing through the cassette to the filter is nearly uniform with no turbulence or vortices; this idealized sampling environment rarely occurs in workplace settings.

The air flow patterns entering an idealized thin-walled sampler have been studied under isoaxial conditions.[2] The fiber sampler inlet falls into the category of thin-walled inlets, which have a wall thickness less than 10% of their diameter. Other studies have considered only overall sampling efficiency for samplers such as the 37-mm open-faced cassette.[3] Sampling efficiency studies of the 25-mm cowled asbestos sampler also have been conducted, though only under stagnant conditions.[4] In a recent review of sampling, Vincent[5] suggests that more research needs to be conducted to elucidate sampling streamlines for inlets, especially at large sampling angles.

A somewhat analogous air-flow situation to sampling at large angles to the local wind direction is the air flow in a pipe bend. It has been observed experimentally[6] and calculated theoretically[7] that a secondary flow pattern consisting of two symmetric vortices is formed, one on each side of the plane of the bend. A similar bend occurs in the flow stream entering the sampler inlet, though the flow is not initially constrained as in the pipe bend. Thus, similar vortices might be expected under anisoaxial sampling conditions.

Several mechanisms of particle deposition have been studied that can contribute to sampler inlet biases: diffusion, impaction, interception, settling, and electrostatic interaction.[5,8] All of these can produce various degrees of sampling biases that depend on the air velocity, direction, and flow pattern in a sampler inlet. Because of the dimensions and typical inlet flow velocities, fiber samplers do not exhibit significant

diffusional losses. The losses due to impaction, interception, and settling have been considered for sharp-edged inlets when the air flow enters the sampler at $\leq 90°$.[9] A semi-empirical theory has been developed that appears to explain inlet losses at these angles adequately. Some research has been conducted to examine inlet losses at larger angles, indicating that inlet efficiencies can be quite variable.[10]

Several studies have evaluated losses of various types of fibers to the inner surface of the inlet or cowl. Some have found a difference between asbestos fiber field measurements with and without a cowl,[11] some have found no difference,[12,13] and others have found significant deposits of refractory ceramic fibers on the cowl.[14] The conflicting results may have several causes. Wang et al.[15] found that when the cassette is not properly sealed, 15–30% of the fibers are lost to the cowl. Comparison of fiber counts on the filter with counts on samples from redeposited cowl washings may be biased, especially when the filters are overloaded.[16]

Johnston et al.[17] investigated the effect of electrostatic-charge induced fiber-sampler losses in workplace samples. Losses were apparent when the sampler was highly charged, but the details of the filter deposit were not observed. Baron and Deye[18,19] investigated electrostatically induced effects under controlled laboratory conditions. They considered particle trajectories and filter deposition patterns for sampling angles near isoaxial conditions. Baron and Deye indicated that the more time a charged particle spent near the outside and the leading edge of the sampler as it entered the inlet, the more likely it was to be affected by coulombic (charged particle, charged sampler) interaction. Filter deposition biases were significant when the particles had the same polarity as the sampler; filter deposition was uniform with little apparent loss when the particles and sampler were opposite polarity.

The effect of wind speed and direction in the neighborhood of a sampler inlet has been emphasized in the evaluation of total[3] or inhalable[20] aerosol samplers. Various wind conditions have been shown to cause large measurement differences with thin-walled cylindrical inlets that are similar to the asbestos sampler.[5] Inertial effects, settling, particle bounce, and resuspension have been indicated as the likely causes of these differences.

Fibers collected from the work environment should be in the size range that might deposit in the lung.[21] The size of aerosol particles that can deposit in the lung, i.e., the thoracic fraction of the aerosol, is defined for sampling purposes in proposals by the International Organization for Standardization and American Conference of Governmental Industrial Hygienists.[20,22] These proposed conventions provide a 50% cut point at 10-μm aerodynamic diameter. Most inertial and gravitational losses increase with particle size. If an accurate sample is collected at 10 μm, then the sampler is likely to be accurate for smaller fibers. Many asbestos fiber diameter distributions measured for workplace aerosols are lognormal with count median diameters that are submicrometer.[23] The aerodynamic diameter of fibers is approximately 3–5 times the physical diameter.[24] Thus, relatively few asbestos fibers that are collected are $>$ 10-μm aerodynamic diameter. However, other types of fibers, such as glass and mineral wool, may have much larger aerodynamic diameters, resulting in more fibers near the cutoff size for thoracic sampling.

The present study was initiated in response to an observation of nonuniform filter deposits in samplers collecting a tungsten carbide dust in an inhalation toxicology chamber.[25] The sampler initially was used for asbestos measurements in these chambers and was applied to the tungsten carbide measurements for consistency. Such nonuniform deposits are the combined result of nonuniform air flow patterns in the inlet under anisoaxial conditions in combination with electrostatic, gravitational, or inertial forces. First, the air flow that produces vortex formation under anisoaxial conditions and at various sampler flow rates is described. This is accomplished from observations of smoke stream patterns and from a new technique for evaluating flow patterns using filter-deposited aerosols. Second, it is indicated how inertial, gravitational, and electrostatic effects combine with vortices within the inlet to produce unique deposition patterns.

EXPERIMENTAL MATERIALS AND METHODS

Three experimental systems were used to observe air flow into the sampler and particle deposition on the sampler filter. In the first system, the flow patterns of air entering an open-faced, 25-mm cassette sampler with a 50-mm long clear-plastic cowl were observed in a horizontal, 24-cm diameter, 100-cm long, clear acrylic tube. The clear-plastic cowl was a special inlet used to visualize the illuminated smoke stream. All other measurements were made with a conductive black plastic cowl.

The air flow entering the tube and surrounding the sampler was conditioned with an open-pore foam (35.4 pores/cm or 90 pores/inch) and a 1.91 cm (3/4") thick aluminum honeycomb flow straightener with 0.318 cm (1/8") diameter hexagonal holes, so that the air flow past the sampler was laminar and uniform. Smoke from a smoke generator was diluted and ducted into the tube as an approximately 2-mm diameter stream. This stream was both isoaxial and isokinetic (14 cm/sec) with respect to the major air flow in the tube. The sampler was placed in the tube at various angles to the air flow, and then the smoke stream entering the sampler was observed. The sampler was illuminated with a high intensity white light source at right angles to the tube axis and the flow patterns were recorded with a 35-mm camera.

The second system consisted of a vertical chamber (1.8 m long, 24 cm diameter) used to observe particle deposition patterns on the 25-mm sampler filter (Figure 1). Particles were generated into the airstream at the top of the chamber from a water solution of methylene blue using a vibrating orifice monodisperse aerosol generator (VOMAG) (Model 3050, TSI, Inc., St. Paul, Minn.); this allowed visual observation of filter deposition patterns. Most of the experiments were conducted with 3-μm aerodynamic diameter particles, except for one using 10-μm aerodynamic diameter particles as indicated.

The VOMAG was modified with a pressure feed system for the liquid and a large reservoir of solution, allowing continuous operation of the generator for several days at a time. The VOMAG was further modified according to the technique

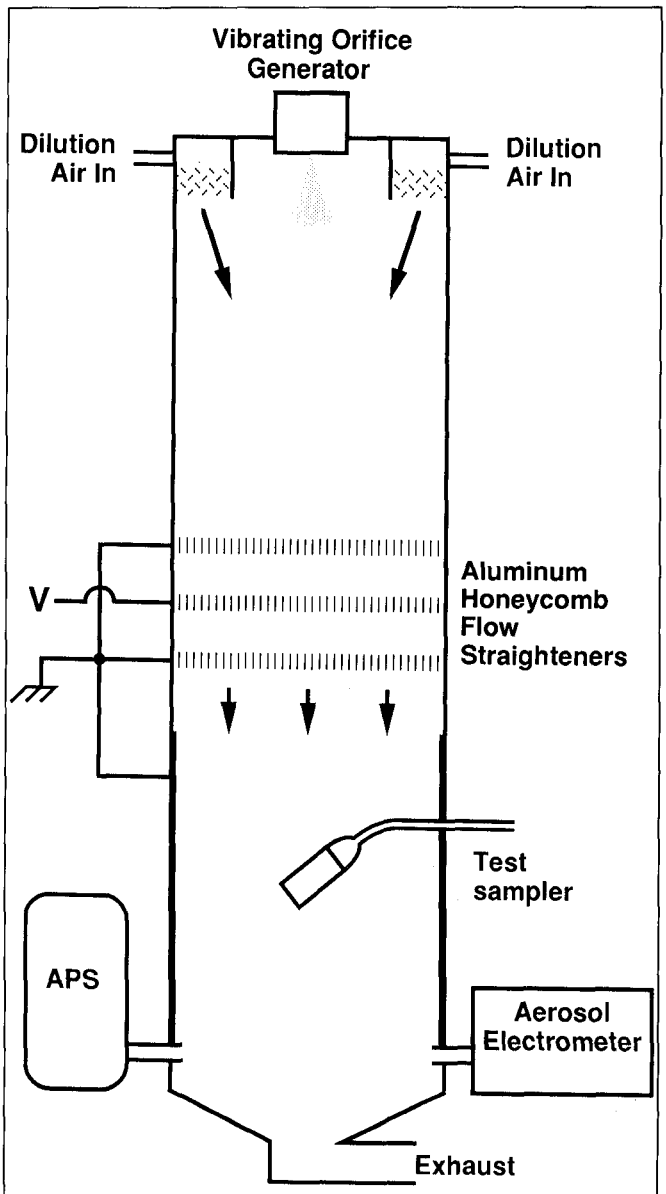

FIGURE 1. Apparatus for detection of flow patterns and electrostatic effects in fiber sampler. Charged monodisperse particles are produced by the vibrating orifice generator. The Aerodynamic Particle Sizer (APS) is used to measure particle size and number while the aerosol electrometer measures total aerosol charge. A potential (V) is applied to one of the honeycomb flow straighteners to induce a hexagonal pattern on the aerosol stream.

of Reischl et al.,[26] whereby a voltage applied to the dispersion-air-orifice plate induced a charge on the droplet stream emerging from the vibrating orifice. The charge on each aerosol particle thus was controlled to have the same magnitude and polarity.

After entering the chamber, the aerosol was diluted and mixed with a concentric sheath flow, allowed to dry, and then passed through three honeycomb flow straighteners (same dimensions as above) situated at 5-cm intervals. The air velocity through the flow straighteners was 14 cm/sec. The sampler was placed 10–30 cm downstream of the last flow straightener. The aerosol particle size and concentration were monitored with an Aerodynamic Particle Sizer (Model APS3300, TSI, Inc. Minneapolis, Minn.). The total aerosol charge was measured using an aerosol electrometer (Model 3068, TSI, Inc.). The charge per particle was calculated using the particle number concentration measured by the APS3300.

All samples were taken using an asbestos filter sampler with a conductive cowl (Millipore Corp., Bedford, Mass.) and a 25-mm, 0.8-μm pore size mixed cellulose ester filter. The deposition patterns of the charged methylene blue particles on the surface of the filter were observed visually. The filters with particle deposits were exposed to heated water vapor to enhance the particle visibility, coated with clear sticky tape, and photographed.

A new method of indicating the flow patterns was used that superimposed a hexagonal pattern on the aerosol stream approaching the sampler. This was accomplished by applying a voltage (± 1000 to ± 3000 V) to the center flow straightener (Figure 1). By choosing the polarity of the voltage so that it was opposite to that of the charged methylene blue particles, the particles were repulsed from the top edges of the final flow straightener and formed a honeycomb pattern. The hexagonal pattern was observed in the filter deposit with the lines indicating an absence of particles. The size and distortion of the hexagonal regions were indicators of the flow trajectories that passed into the sampler. Both the sampler and the chamber surrounding it was grounded so that charged particles entering the sampler would not experience any electrostatic field. An image analysis system (Magiscan 2, Applied Imaging, Tyne & Wear, U.K.) was used to measure hexagonal areas of particle deposit on the filters.

The air velocity in the chamber was set using a thin film anemometer (model 441, Sierra Instruments—now Graseby Andersen, Atlanta, Ga.). However, the velocity was measured by comparing the hole size in the flow straightener with the filter deposits for isoaxial samples as described below.

The electrostatic effects on sampled particles were observed by sampling the charged methylene blue particles with the sampler attached to a high voltage power supply (0–20,000 V). For these experiments, the hexagonal pattern was not imposed on the aerosol stream ($V = 0$, Figure 1) since it interfered with the observation of electrostatic sampling effects. The inner walls of the test chamber below the flow straighteners were covered with aluminum foil tape and grounded. The deposit on the filter provided an indication of the electrostatic effect and was photographed in the same manner as indicated above. Similar experiments were conducted with uncharged aerosol particles, and with sampler and chamber grounded to evaluate inertial and gravitational effects.

In a third system, used to demonstrate nonuniform particle deposit under less controlled conditions, a tungsten carbide aerosol was generated using a modified Wright dust feeder[27] and introduced into a horizontal inhalation toxicology chamber.[25] The carrier flow through the dust feeder was 7 L/min dry air. The air flow through the chamber was 0.32 m^3/min; chamber temperature was nominally 21 °C; and relative humidity ranged from 50–72%. The air flow through the chamber was characterized with a hot wire anemometer to indicate the velocity and approximate direction of the flow. The

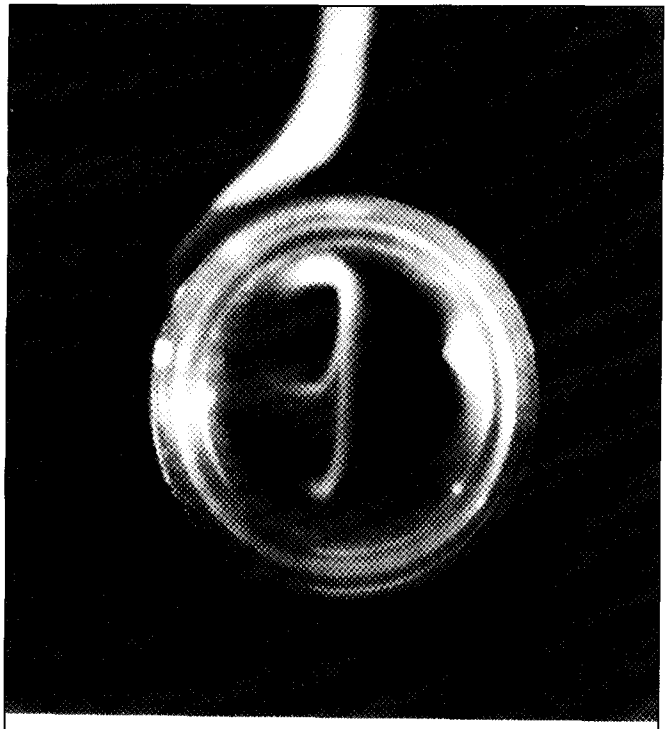

FIGURE 2. Flow pattern produced by smoke stream entering asbestos sampler in an axial view of the sampler at chamber air velocity of 14 cm/sec and inlet flow velocity 16 cm/sec (flow rate 5 L/min). The sampler axis is about 120° to the chamber air flow.

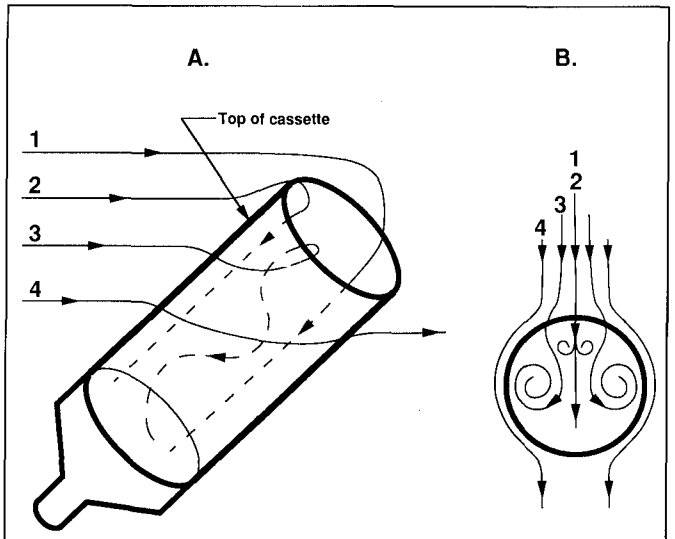

FIGURE 3. A: Schematic of flow streamlines entering an asbestos sampler at high angle. The top of the cassette is the line running along the cowl parallel to the sampler axis on the upstream side. B: The same flow paths viewed along the sampler axis. Note that the vortex paths may be more complex and rotate in a different direction depending on flow rate and sampling angle.

aerosol was sampled using the 25-mm cassette with conductive cowl, at several angles to the air flow in the chamber. The air sampling flow through the cassettes was approximately 1 L/min. The voltage on the cassettes was measured with an electrometer (model 610B, Keithley Instruments, Cleveland, Ohio). The size distribution of the tungsten carbide aerosol was measured with an eight-stage cascade impactor (model 216, Sierra Instruments—now Graseby Andersen, Atlanta, Ga.).

RESULTS

The highest flow rate typically used for fiber sampling with the 25-mm cassette is 10 L/min, resulting in a Reynolds number of 550. The chamber flow (Figure 1) was also in the laminar range with Re = 1200. However, workplace air may exhibit a large range of conditions, from stagnant to much higher velocities than in the sampler inlet. This study covers the range of inlet velocities typically used with the fiber sampler and a single external chamber air velocity of 14 cm/sec. The sampling velocity ratio (ambient air velocity divided by inlet air velocity) covers the range of 0.44–8.7. Completely stagnant ambient air is expected to produce smooth air flow into and through the inlet, while high ambient velocities, especially with turbulence, may cause complex flow patterns within the inlet. The vortices observed in this study are still laminar; they also may cause problems for fiber sample analysis, or potentially cause inertial losses onto the inlet walls.

The air flow streamlines entering the 25-mm cowled sampler were made visible with smoke, an example of which is shown in Figure 2. In general, though the smoke stream could be readily observed, good photographic records of the three dimensional flow patterns were difficult to obtain. The cassette axis was oriented at a series of angles between 0° and 180° to the flow axis. Some general trends in the flow streamlines were observed. These can be summarized using Figure 3 as an aid to visualization of the flow streamlines. At angles lower than about 60°, the flow into the entire inlet was uniform and laminar as indicated by Streamlines 1 and 2. At larger angles, two sets of vortices were formed, one on each side of the inlet, with a plane of symmetry containing the axis of the sampler and the direction of chamber air flow.

The shape of the vortices was complex and varied with angle and flow rate. As indicated in Figure 3, the part of the sampler inlet located furthest upstream to the chamber flow was designated the top of the sampler. At higher flow rates, the vortices had smaller diameters and were concentrated near the top of the inlet. At lower flow rates, e.g., 2 L/min, the vortices filled the entire cross section of the inlet. Note that at angles greater than 90°, the flow streamlines entering the inlet were split and traveled along the outer surface of the cowl, entering the cowl inlet near the leading surface of the cowl (Figure 3, Streamline 3).

As described in the Experimental Materials and Methods section, a new technique was developed that allowed deduction of the flow pattern from the filter deposit. The technique superimposed a hexagonal pattern onto the aerosol flow. These patterns are shown in Figure 4 for isoaxial sampling at four flow rates. Area measurement of the individual hexagonal areas of isoaxial samples with the image analyzer gave results with a 5–10% relative standard deviation for a single filter. The areas of the hexagons were inversely proportional to the

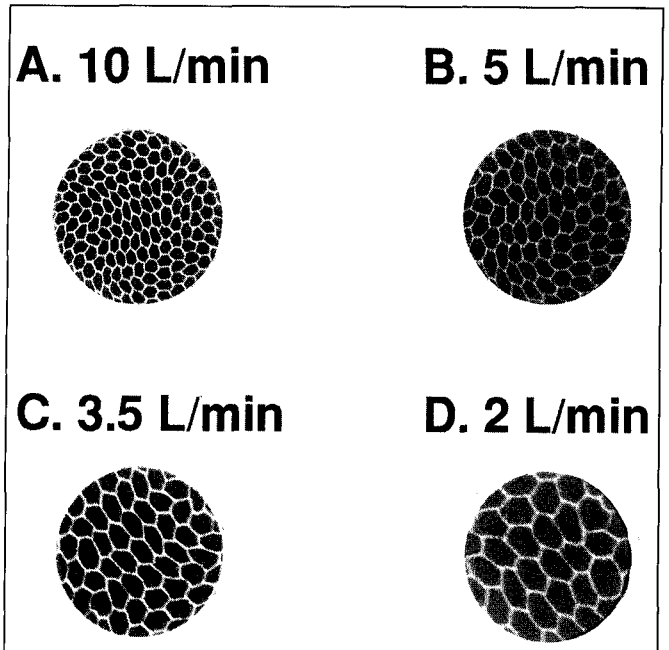

FIGURE 4. Filter deposition patterns produced from an aerosol stream of 3-μm methylene blue particles with a hexagonal pattern superimposed. Aerosol stream velocity is 14 cm/sec and sampling is isoaxial at velocities of A: 32 cm/sec (10 L/min); B: 16 cm/sec (5 L/min); C: 11 cm/sec (3.5 L/min); and D: 6.4 cm/sec (2 L/min).

flow rate into the inlet. Note that most cowls are slightly tapered; the mean inlet velocity was calculated using the diameter at the front of the inlet and not at the filter surface. The mean areas of the hexagonal regions in Figure 4 were measured with the image analysis system and plotted against the sampler flow rate (Figure 5). The imprint of the honeycomb flow straightener also was measured with the image analyzer and the mean hexagonal area used to estimate the air velocity in the chamber (14 cm/sec).

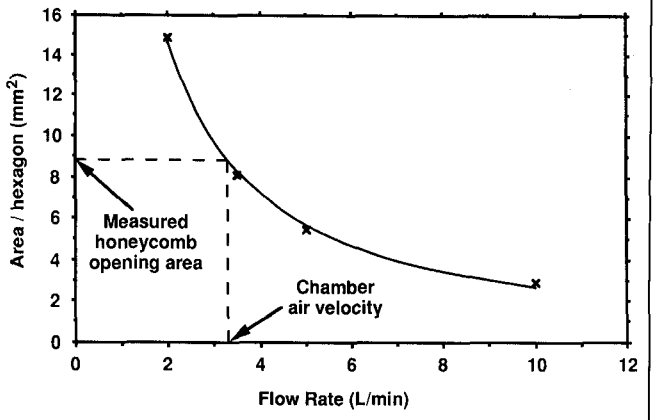

FIGURE 5. The measured flow rate through the sampler compared to the mean hexagonal area on the filter under isoaxial sampling conditions. Solid line = regression of mean hexagonal area against inverse of flow rate. Measured size of flow straightener opening allows estimation of chamber air velocity through flow straightener.

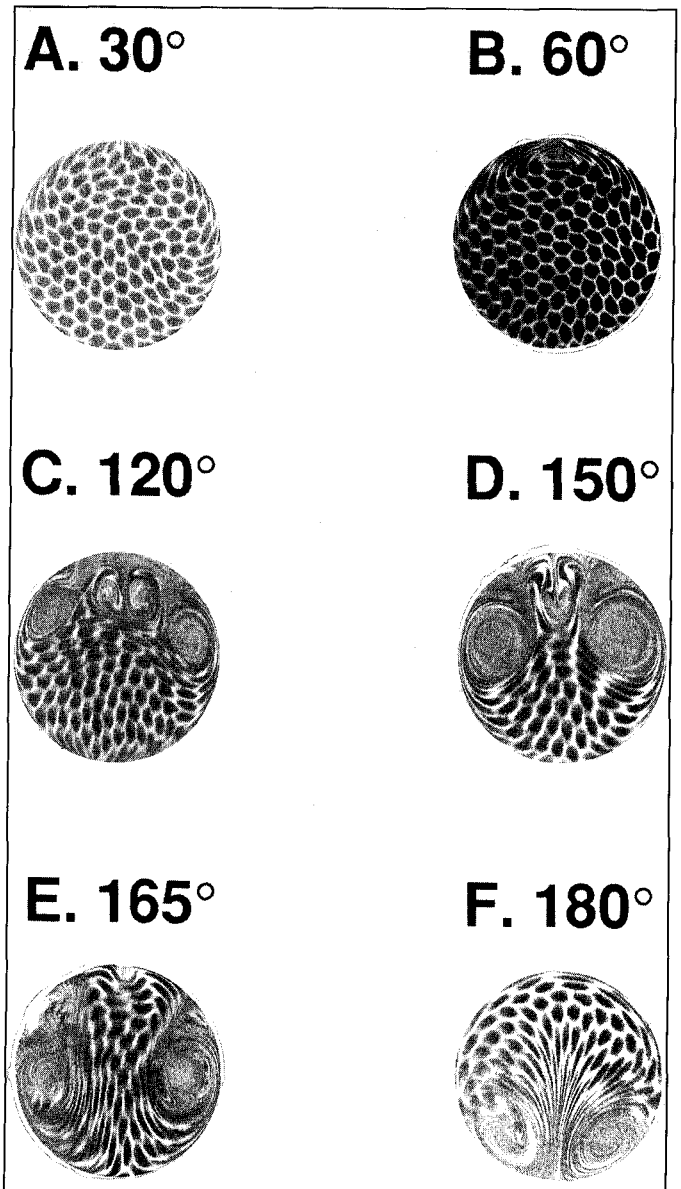

FIGURE 6. Filter deposition patterns produced when sampling 3-μm methylene blue particles from a 14 cm/sec aerosol flow (hexagonal pattern superimposed) with an inlet velocity of 32 cm/sec at the angles A: 30°, B: 60°, C: 120°, D: 150°, E: 165°, and F: 180°. Distortion of flow indicated by distortion of hexagonal pattern originally imposed on aerosol stream.

Figure 6 shows filter deposits observed at 10 L/min (32 cm/sec inlet velocity) for a range of angles from 30° to 180°. Figure 7 allows comparison of filter deposits at two angles and three flow rates.

Figure 8 depicts measurements taken at a 120° sampling angle with larger uncharged particles (10 μm) over a range of flow rates from 0.5 to 10 L/min to indicate the importance of gravitational and inertial forces in the vortices. For the 0.5-L/min sample (Figure 8D), measurement of the area covered

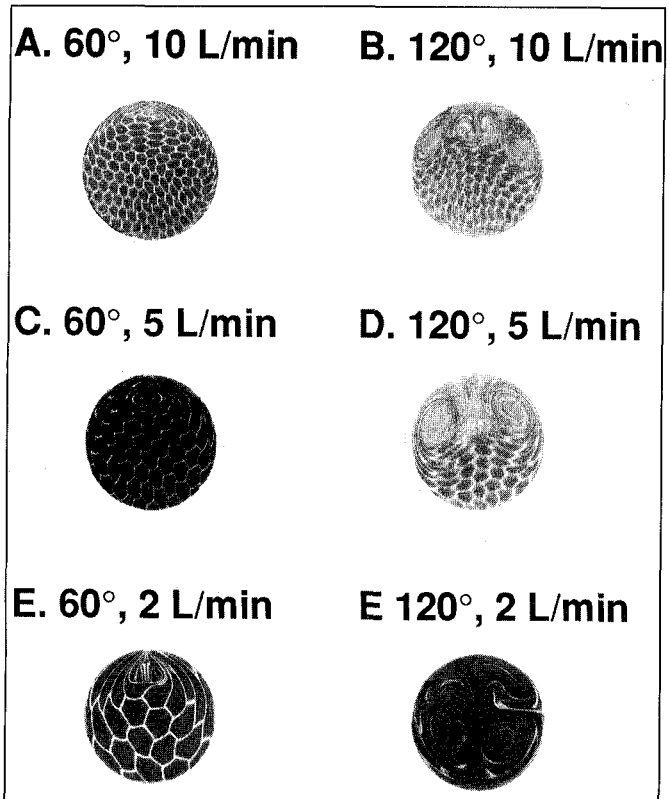

FIGURE 7. Filter deposition patterns produced when sampling 3-μm methylene blue particles from a 14 cm/sec aerosol flow (hexagonal pattern superimposed) with an inlet velocity of 32 cm/sec (10 L/min); 16 cm/sec (5 L/min); and 6.4 cm/sec (2 L/min) at sampling angles of 60° and 120°.

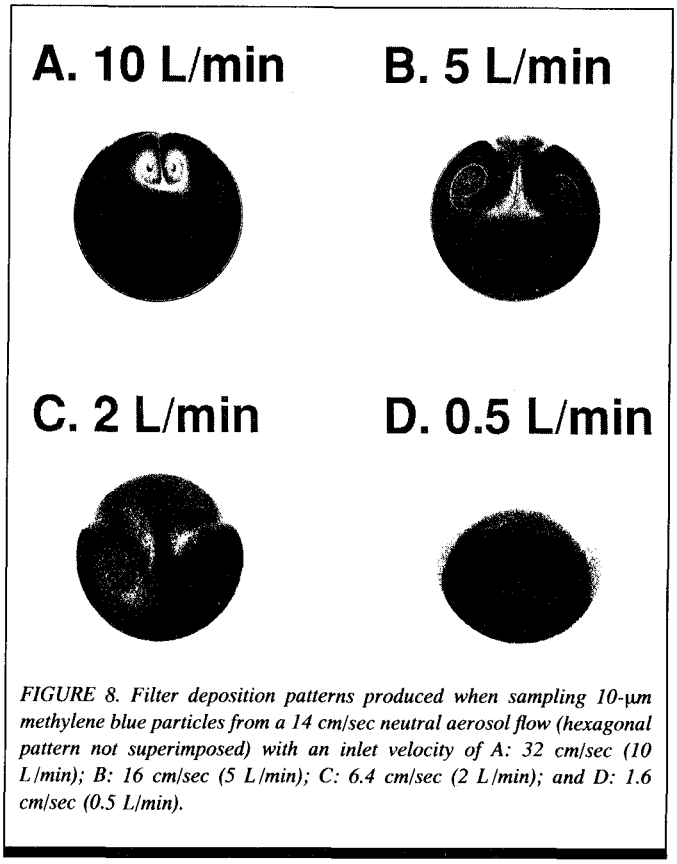

FIGURE 8. Filter deposition patterns produced when sampling 10-μm methylene blue particles from a 14 cm/sec neutral aerosol flow (hexagonal pattern not superimposed) with an inlet velocity of A: 32 cm/sec (10 L/min); B: 16 cm/sec (5 L/min); C: 6.4 cm/sec (2 L/min); and D: 1.6 cm/sec (0.5 L/min).

by the methylene blue deposit indicated that 72% of the particles reached the filter. This deposit is consistent with previous measurements of inlet losses due to settling onto the inlet surface. The vortices caused only slight mixing of the aerosol within the cowl at this flow rate, as evidenced by the slight shading on either side of the heavier deposit.

The results of electrostatic effects as a function of particle/sampler charge and of flow rate can be noted in Figures 9 and 10, respectively. Samples of 3-μm methylene blue particles carrying approximately 500 charges (electrical mobility = 0.5 cm^2/statV-s) were taken at 10 L/min with a 120° sampling angle. The sampler was set to voltages ranging from 0 to 4000 V. The electrical field experienced by particles entering the sampler could not be measured accurately because of the complex geometry of the sampler/chamber configuration. The leading edge of the sampler (oriented 120° to the air flow) was situated approximately 4.5 cm from the grounded cylindrical chamber wall (See Figure 1).

Only sampling situations where the polarity of the particles and sampler were the same produced a noticeable particle loss and pattern on the filter surface. All patterns noted here are the result of measurements with the particle charge and sampler voltage having the same polarity. Other measurements indicated that the product of sampler voltage and particle charge correlated well with specific patterns, i.e., a decrease of one of these two parameters could be compensated by a proportionate increase in the other parameter. The effect of sampling flow rate is indicated in Figure 10 for a particle charge of 500 e, the sampler charged to 500 V and oriented 120°, and flow rates of 10 L/min, 5 L/min, and 2 L/min.

To demonstrate that the sampling effects observed in the laboratory could occur under less controlled conditions, a series of samples were taken in the inhalation chamber, resulting in observable filter patterns. The size distribution of the tungsten carbide aerosol was 1.7 μm with a geometric standard deviation of 1.4. Examples of these patterns are given in Figure 11. The indicated sampling angle of 160° assumes that the local ambient flow past the sampler was horizontal. Under normal operating conditions, the patterns could not be repeated consistently and were probably affected by the humidity of the generation system air. The effects were noted during the winter when indoor air humidity was low and disappeared during the spring and summer when the humidity was higher. The lower humidity apparently affected the dispersion air in the generator, producing a more highly charged aerosol. Additional measurements in which the generated aerosol and the sampler were deliberately charged confirmed that electrostatic effects were the likely cause of the observed patterns.

DISCUSSION

Flow Patterns

There has been little discussion in the literature regarding patterns of air flow entering samplers at high angles. The present study was initiated to explain filter deposition patterns ob-

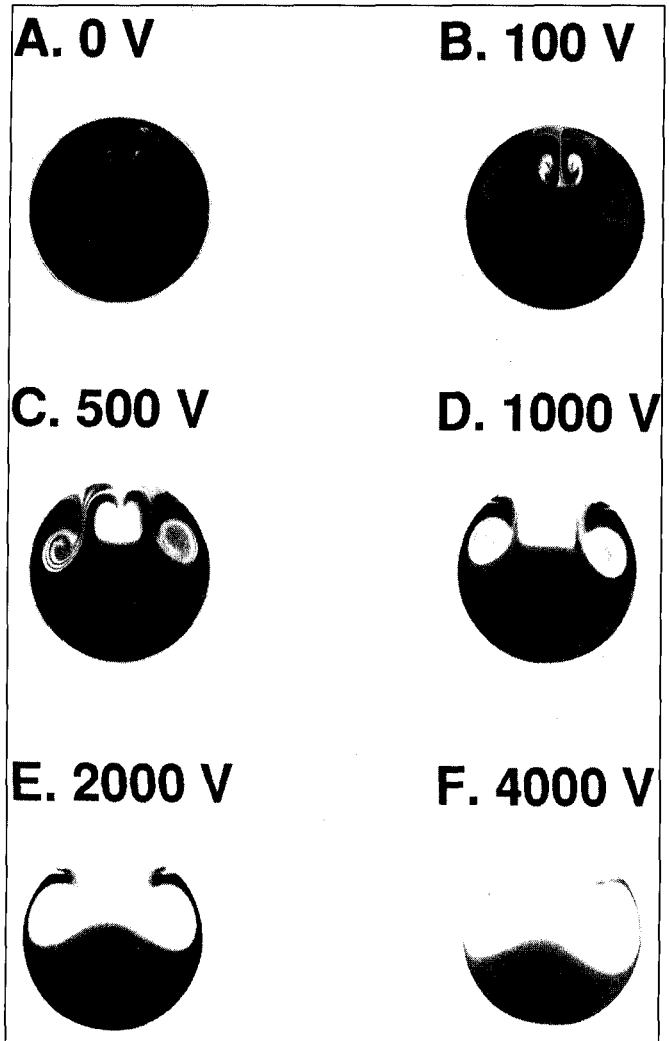

FIGURE 9. Filter deposition patterns produced when sampling charged 3-μm methylene blue particles from a 14 cm/sec aerosol flow (hexagonal pattern not superimposed) at a sampling angle of 120° with an inlet velocity of 32 cm/sec (10 L/min). Particle charge is 500 e. Sampler voltage set at levels indicated.

served under these conditions. While the smoke stream observations allowed visual inspection of the air stream lines entering the sampler, the smoke streams were difficult to record and quantitate. The second technique for identifying the flow patterns within the sampler was to observe the distortion of the hexagonal pattern imposed on the aerosol stream. While this did not allow direct visualization of the flow itself, it did allow a more sensitive indication of distortions in the flow as well as a more quantitative indication of vortex size and complexity. The air velocity in both 24 cm diameter measurement chambers was 14 cm/sec. The samplers were operated over a range of angles between 0–180° and inlet velocities between 1.6–32 cm/sec. These velocities corresponded to the typical sampler operating range of 0.5 to 10 L/min.

The smoke stream chamber was used to observe the flow outside and entering the inlet. At small angles (0° to 60°) with the cassette pointing into the air stream, no vortices were observed in the patterns entering the sampler. At an angle of about 90°, a small vortex was observed on each side of the inlet. As the angle increased, the vortices grew and became more complex. At high velocities, the vortices were positioned near the top of the cowl. As the velocity decreased, the vortices grew larger and shifted away from the top of the cowl. Figure 3 is a schematic of air flow approaching and entering a cassette at about 120° to the axis of the cassette.

The second chamber (Figure 1) allowed more quantitative comparison of the cross-sectional area covered by the vortices and smooth flow. The isoaxial (0°) deposition measurements (Figure 4) indicated that the variability of the hexagonal areas on the filter had a relative standard deviation of 5–10%. Some of this variation may have been due to the area measurement technique, some to variations in flow through the filter (from differences in filter uniformity), some to distortions in the hexagonal structure of the honeycomb, and some to the variation in flow through the flow straightener. The latter occurs because the flow straightener removes lateral flow variation but not necessarily the variation parallel to the flow direction. A screen with a higher pressure drop placed upstream of the flow straighteners might improve the uniformity, but also would increase the loss of particles in the system.

The particle-free regions of filter deposit represented the set of streamlines that had started at the hexagonal edges of the flow straightener and ended at the filter surface. Sampling theory for sharp-edged inlets predicts that the number of streamlines entering the inlet is uniform and inversely proportional to the flow rate.[2] The velocity distribution is constrained to be uniform at the sampler filter surface due to the equalizing influence of the pressure drop across the filter. The average measured area within each deposited hexagonal region is inversely proportional to the flow rate through the sampler. The hexagonal regions appear to be the same average size over the entire surface of the isoaxial samples.

The comparison of the mean hexagonal areas on the filter (from Figure 4) with the area of the openings in the flow straightener allowed the estimation of the flow rate in the chamber region where the sample was taken (Figure 5). The precision for this technique for measuring air velocity was limited primarily by the accuracy of the flow rate in the sampler. The sampler flow rate was set with a rotameter that was calibrated against a bubble meter. The rotameter setting was accurate to only about 5%. The hexagonal area measurements from the filter and the flow straightener were repeatable to better than 1%.

Figures 4 and 6 depict the patterns observed in isoaxial and anisoaxial inlet configurations, respectively. The sampler was operated at 10 L/min at angles of 0°, 60°, 120°, 150°, and 180°. At 60° the first vortices began to form. At 120° the vortices were more fully developed, and a second set of vortices formed at the sides of the initial vortices. At about 165° the first pair of vortices disappeared, and the second set moved to the sides of the inlet. At 180° the uniform flow region broadened, but there was still a pair of vortices quite evident. The vortices were on the same side of the inlet as the tube providing the suction for the sampler. It could be argued that the deposition pattern for 180° sampling should be symmetric (similar to 0° sampling) since the sampling is isoaxial. How-

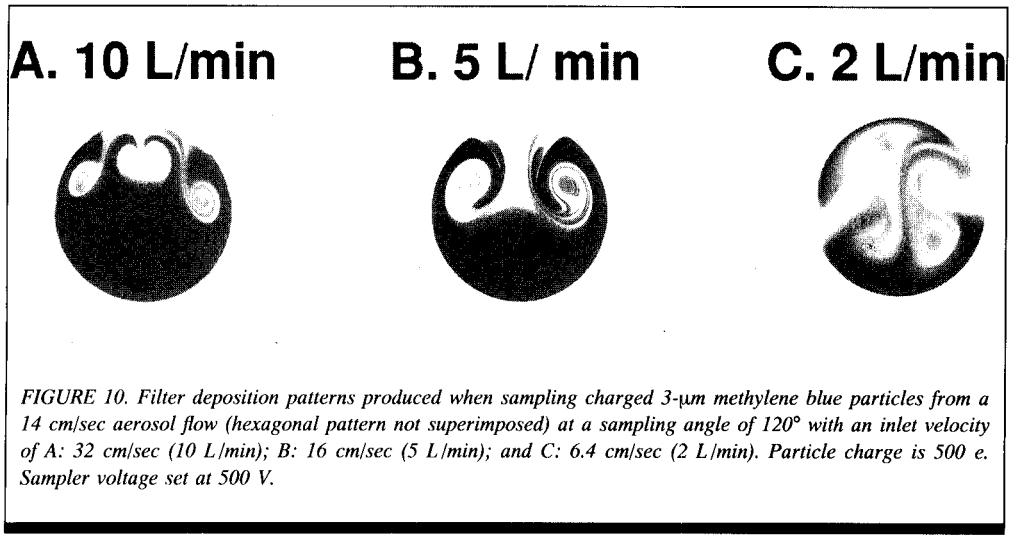

FIGURE 10. Filter deposition patterns produced when sampling charged 3-μm methylene blue particles from a 14 cm/sec aerosol flow (hexagonal pattern not superimposed) at a sampling angle of 120° with an inlet velocity of A: 32 cm/sec (10 L/min); B: 16 cm/sec (5 L/min); and C: 6.4 cm/sec (2 L/min). Particle charge is 500 e. Sampler voltage set at 500 V.

ever, the tube providing the sampler suction remained as an obstacle to complete axial symmetry, apparently causing the observed vortices.

The deposition patterns displayed in Figure 7 indicate that the vortices formed at a specific angle were similar regardless of the inlet flow rate. The flow rate only affected the size of the lateral extent of the vortices, not their basic shapes. Further, the second set of vortices were formed at an angle just below 90° and thus may be due to the splitting of flow at the plane of symmetry of the sampler at higher angles, as indicated by Figure 3, Streamline 3.

The vortices or secondary flow patterns that are formed in the inlet do not necessarily produce a nonuniform pattern on the filter surface. Only when an inertial, gravitational, or electrostatic force becomes important are the vortices made visible. In addition, the location and mechanism of particle motion determine which parts of the vortices are made visible.

The measurements carried out in this study were performed largely with compact or spherical particles. However, the conclusions are applicable to fibrous aerosols, since the inertial, gravitational, and electrostatic forces on fibers under most sampling conditions are very similar to compact particles of the same aerodynamic diameter.

Inertial Effects

The presence of the vortices does not necessarily affect the sampling accuracy, i.e., the loss of particles to the wall of the cowl. The inertial forces within a vortex will cause particles to be transported laterally away from the center of the vortex. For the 3-μm particles this lateral transport appears to be noticeable though relatively small, as indicated by the small particle-free spots in the center of the vortices at 120° sampling angle, 10-L/min inlet flow (Figure 9A). The lateral motion appears to be less than 1 mm. However, measurements with 10-μm particles indicate greater lateral transport of the particles as indicated by the clearly observable vortex patterns in Figure 8A. The inertial force thus appears to increase with higher sampling rate and correspondingly larger tangential vortex flow as well as larger particle size, resulting in a larger particle-free region. However, gravitational effects also increase with particle size, and the amount of lateral transport in Figure 8A due to inertial force versus gravitational force is not clear for the 10 L/min samples.

In addition to the lateral transport of particles by the vortices, the sharp bend in the air flow at the inlet face (Streamline 1, Figure 3) also may cause nonuniform particle trajectories. This creates a particle-free region on the upstream side of the inlet that would be mixed by the vortices. For instance, the pattern in Figure 8A may be due primarily to this inertial effect combined with the vortices.

The observation of inertial modification of the filter deposit indicates the possibility of enhanced deposition on the cowl wall. Measurements on laminar flow in 90° pipe bends, which induce vortices similar to those observed here, indicate that inertial losses < 2% are expected for particles up to 10-μm aerodynamic size.[28] The wall losses in such bends increase with flow rate, bend angle, and particle size. By analogy, one would expect increases in cowl-wall deposition as a function of the same parameters.

The ambient air velocity was not changed in the present study due to limitations in the chamber, but also may have a significant effect on the inertial forces in the vortices. The ambient air velocity of 14 cm/sec is low compared to many workplace velocities, which can range more than two orders of magnitude higher. The empirical sampling theory developed by Hangal et al.[9] indicates that inertial losses increase with increasing external wind velocities at sampling angles up to 90°. In addition to inertial losses caused by bending the air stream, it may be that increasing the external air velocities results in higher vorticity at large sampling angles, further enhancing inlet surface (cowl) deposition.

Gravitational Effects

Gravitational settling has been considered for thin-walled inlets sampling at < 90° to the wind velocity[9] and for pipes at various angles.[29] The sample taken at 120°, 0.5 L/min (Figure 8D) clearly indicated that at low inlet flows settling plays a major role in filter losses, increased cowl deposit, and filter nonuniformity. The percent area covered by particle deposit (72%) agrees well with the 67% predicted[29] for a 2.5-cm diameter, 5-cm long pipe inclined at 120° to the vertical (30° to the horizontal). Increasing the sampling angle to 150° (60° to the horizontal) increases the percent area covered to 78%. In this range, the losses are not a very sensitive function of the sampling angle. The orientation of the sampler on an erect mannequin is approximately 137° (47° to the horizontal).[3]

Gravitational settling rate increases with particle size, indicating that large particles are sampled inefficiently at low inlet flow rates. Again, for asbestos fibers with diameters smaller than 1 μm (approximately 3–5 μm aerodynamic diameter), this may not be a problem. However, for larger diameter fibers such as fibrous glass, significant loss to the cowl and filter deposit nonuniformity will occur. These effects will be strongly dependent on flow rate and on sampler angle relative to the gravitational force.

Electrostatic Effects

The electrical field surrounding a sampler produced by charges on the sampler itself or on nearby objects can affect the trajectory of particles approaching and entering the sampler. In the experimental configuration indicated in Figure 1, the highest electric field region near the sampler occurs at its top leading edge because this is the point closest to the grounded surface, and because the surface curvature is the highest. The electrical field surrounding the sampler is relatively complex because of the asymmetric orientation of the sampler relative to the surrounding chamber. The high field region around the inlet in the chamber is somewhat analogous to the high field region near the sampler when worn by a worker, since the sampler protrudes from the worker's body. A calculation of the electric field near the surface of the sampler indicates that the field is relatively insensitive to the distance of the grounded surface from the sampler. Thus, the electric field near the sampler when the grounded surface is 50 cm from the sampler inlet is about 20% lower than with the 10 cm spacing between the sampler and chamber wall. This indicates that the electric field near the sampler is primarily determined by the charge on the sampler and only secondarily on the distance from another charged or grounded surface.

When the electrical polarity of the aerosol particle is different from that of the sampler, particles are attracted to the sampler surface; however, additional particles are attracted from the air stream and the net deposit on the filter is uniform and appears virtually identical to that occurring in the absence of charge effects. Further work is needed to quantitate losses under these conditions. When the polarities of the particles and sampler are the same, particles are repelled from the surface and leading edge of the inlet. At relatively low particle charge/sampler voltage, this results in a narrow semicircular region of particle-free air entering the inlet near its top edge. At much higher charge levels, the particles may be completely repelled from the sampler. The effect of particle/sampler polarity is similar to that noted by Baron and Deye[19] for isoaxial sampling. With this more symmetric situation, particle loss occurs around the entire circumference of the inlet for the same polarity case and no losses occur for the opposite polarity case.

As also noted by Baron and Deye,[19] the faster a particle moves past the outer surface and leading edge of the inlet, the smaller the effect of electrostatic interaction. This point is confirmed in Figure 9, where the losses, as indicated by the particle-free areas on the filter, increase with decreasing flow rate. The electric field surrounding the sampler in the chamber experiments was affected by the closeness of the grounded chamber wall to the sampler. In most workplace sampling situations the sampler is likely to be much further from a grounded surface, and the electric field surrounding the sampler will be smaller for the same level of sampler charge.

Interaction of Air Flow with Various Forces

As indicated above, the deposit of particles on the filter can be uniform even in the presence of secondary flow vortices if the inertial, gravitational, and electrostatic forces are negligible. Each force can combine with the vortices in a unique fashion to produce a nonuniform deposit. The forces shift the spatial distribution of particles entering the sampler and create a particle-free region of space. The deposition pattern due to the inertial effect is likely to be observed only in the regions of highest angular velocity in the vortices. These effects will therefore show up only in the center portion of the most intense vortices. The observed deposit pattern due to settling effects occurs because of the particle-free region formed inside the cowl as the aerosol particles settle. This particle-free region is negligible at the inlet and becomes larger linearly along the length of the inlet. In contrast, the electrostatic repulsion of particles occurs outside the inlet and is likely to create a particle-free space near the edge of the inlet. The final deposit depends on how the particle-containing and particle-free regions are distorted by the vortices.

Sampling for asbestos and other fibers is conducted under two principal conditions: personal sampling for determining worker exposure, and area sampling for determining cleanliness of an abatement operation. Personal samplers are placed in the breathing zone, usually on the chest, with the inlet facing slightly forward. For instance, Buchan et al.[3] used a sampling angle of 47° to the horizontal in their mannequin studies of personal samplers. When ambient air approaches the worker from the front, the air is affected by the worker's body and passes the sampler at angles smaller than 90°. However, if the air comes from behind the worker or from above the worker, the air flow may pass the sampler at angles larger than 90°. The variability of the air-flow direction may serve to average out the deposition patterns over a period of time, reducing the overall variability on the analyzed sample.

However, if the worker is downstream of a fiber source and spends a significant portion of time in a fixed relationship to that source, a relatively well-defined pattern of fiber deposit may develop on the filter. If the sampler is placed at a fixed site to obtain an area sample, the relationship to the aerosol source is further constrained, increasing the likelihood of patterns developing on the filter surface. The degree of complexity in real sampling situations is likely to be great and it is difficult to predict the degree of variability contributed by the vortices combined with inertial, gravitational, and electrostatic effects in the current sampler.

An area sampler is usually situated at a height of 1–2 m with the inlet facing downward. Since air flows in indoor environments are frequently horizontal or downward-directed (from ceiling ducts), the inlet sampling angle is likely to be 90° or greater. The comments regarding personal sampling can

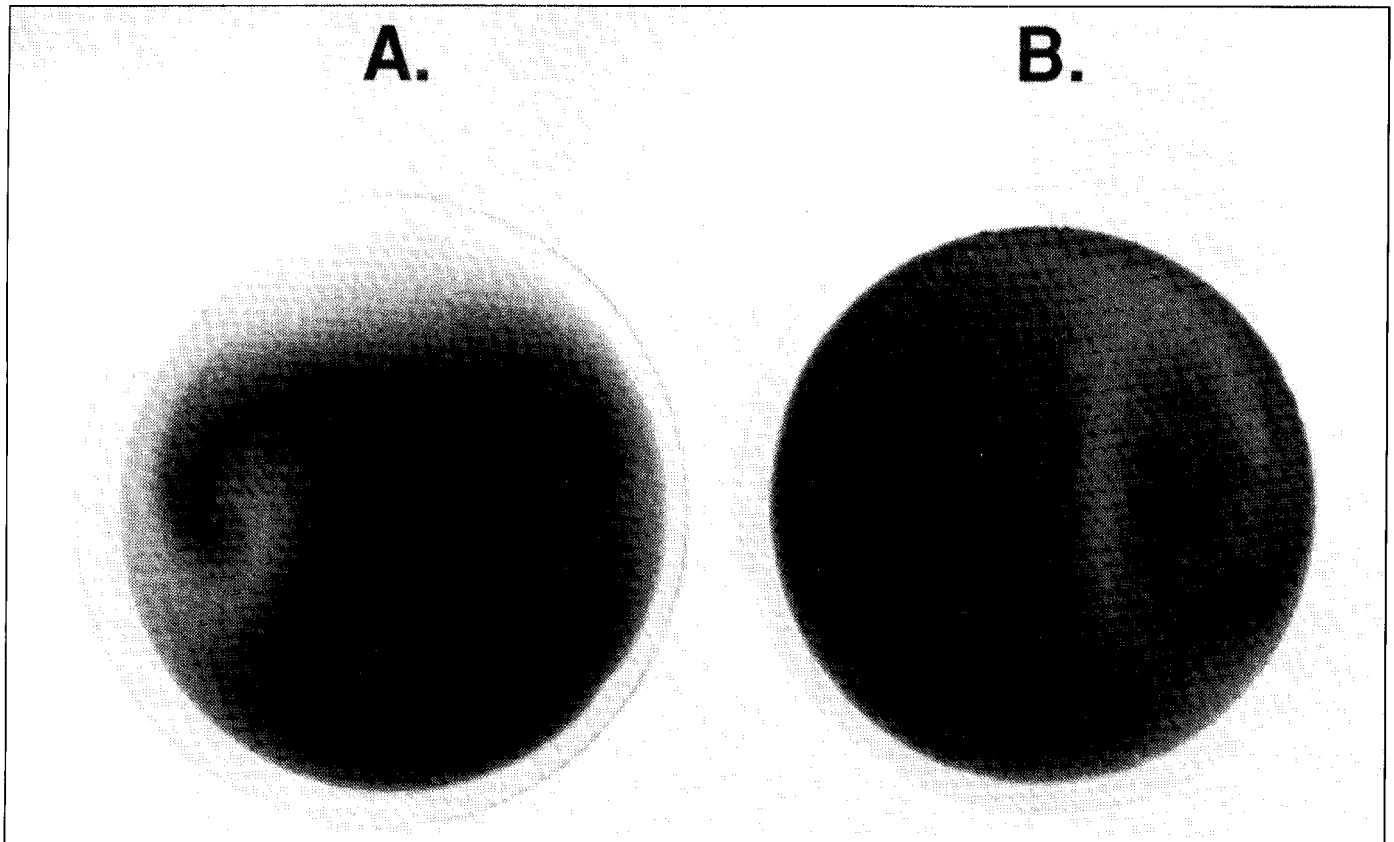

FIGURE 11. Two filter deposition patterns of tungsten carbide aerosol (mass median aerodynamic diameter = 1.7 μm; s_g = 1.4) observed in a horizontal toxicology chamber. A: 160° sampling angle, 1.1 L/min.; B: 160° sampling angle, 0.70 L/min.

apply here in that a bluff body or plate shielding the sampler from large angle air flows could readily be constructed. However, these suggested modifications may result in biases and need to be thoroughly tested before implementing widespread changes in the sampler and sampling protocol.

In each of the controlled experiments described here, tests were conducted with monodisperse test particles carrying identical charge levels. The ambient air velocity in the chamber was fixed at 14 cm/sec. The patterns were sharp and clearly observable. With a workplace aerosol, the particles typically exhibit a lognormal size distribution and might be expected to carry a range of charges with a distribution centered on zero charge[17] In addition, the workplace aerosol is often the result of a mixture of dust particles from different sources and with different electrical properties. Finally, the ambient air velocity can fluctuate significantly. Thus, the patterns observed here due to the electrostatic interactions may not be as clearly observable under field conditions.

However, measurements of the polydisperse tungsten carbide aerosol indicate that nonuniform patterns can be observed clearly under the right conditions. The particles in this aerosol were too small to exhibit significant inertial or gravitational effects. Although some efforts were made to reduce electrostatic effects, e.g., conductive sampler and grounded surroundings, sufficient charge remained on the aerosol and sampler to produce a particle-free pattern on the filter surface. Thus, the various forces described can contribute significantly to the nonuniformity of the filter deposit and, hence, increase measurement variability and bias.

The experiments described here have been performed with spherical or compact particles. Fibers may become aligned in shear flow fields or in electrostatic fields, but their behavior under gravitational, inertial, or electrostatic forces will be similar to that of compact particles with the same aerodynamic diameter and charge level. However, fibers generated under workplace conditions may tend to carry larger charge levels than similarly generated compact particles and thus be prone to larger electrostatic effects.

Implications for an Improved Fiber Sampler

The combined flow patterns and losses noted here suggest several possible changes to the current fiber sampler. First, these effects occur primarily at large sampling angle. If the inlet of the sampler pointed straight out from the worker's body, the range of air flow angles around the inlet would be reduced by the body's shielding. This approach has been implemented in the inhalable aerosol sampler developed at the Institute of Occupational Medicine (IOM).[30] The IOM sampler is fixed on the worker with the inlet pointing perpendicular to the body surface, so that sampling at angles larger than about 90° is prevented. For area sampling this plate might be made larger to further narrow the range of sampling angles toward the forward direction.

The vortices form at the front surface of the inlet and propagate down the length of the cowl. With a shorter cowl, the number of vortex turns within the cowl are reduced. This would further reduce the complexity of the deposition pattern. An alternative is to place a flow straightener, such as a section of honeycomb or open-pore foam, at the inlet. These devices will cause some fiber losses but may improve the overall performance of the sampler.

At 0.5 L/min and a 120° sampling angle, approximately 30% of 10-μm particles settle on the cowl before they reach the filter. Therefore, under these conditions the current sampler acts almost like a sampler for thoracic aerosol. With an appropriate sampler design, including a preclassifier, the sampler would act like a thoracic sampler under all conditions and provide more reproducible results. Open-pore foams have been used as thoracic preclassifiers and are likely to produce a more uniform deposit on the filter surface.[31] A different pore size and/or foam thickness is needed for each flow rate. However, such an inlet would reduce the effects of the vortices and of the settling as a function of flow rate.

CONCLUSIONS AND RECOMMENDATIONS

Improved understanding of the air flow patterns surrounding and entering a sampler may result in the design of a more accurate sampler and implementation of an appropriate sampling protocol. The fiber sampler is likely to benefit from such a redesign. When sampling at large angles to the local air velocity, the uniformity of fibers on a filter sample may be degraded by a combination of air flow patterns and inertial, gravitational, and electrostatic effects. The factors for reducing electrostatic sampling effects under isoaxial sampling conditions as discussed by Baron and Deye[18] are applicable here as well (e.g., higher sampling rates produce fiber deposits that are less biased). It may be possible to redesign the fiber sampler to reduce the sources of measurement error noted in this study. A modified fiber sampler with an inlet similar to that of the IOM inhalable aerosol sampler is suggested, but any changes to the current sampler will need to be carefully evaluated prior to implementation.

REFERENCES

1. **Carter, J., D. Taylor, and P.A. Baron:** Fibers, Method 7400 Revision #3: 5/15/89. In *NIOSH Manual of Analytical Methods.* P.M. Eller, ed. Cincinnati OH: Department of Health and Human Services, National Institute for Occupational Safety and Health, 1984.
2. **Belyaev, S.P. and L.M. Levin:** Techniques for collection of representative aerosol samples. *J. Aerosol Sci. 5*:325–338 (1974).
3. **Buchan, R.M., S.C. Soderholm, and M.J. Tillery:** Aerosol sampling efficiency of 37 mm filter cassettes. *Am. Ind. Hyg. Assoc. J. 47*:825–831 (1986).
4. **Beckett, S.T.:** The effects of sampling practice on the measured concentration of airborne asbestos. *Ann. Occup. Hyg. 21*:259–272 (1980).
5. **Vincent, J.H.:** *Aerosol Sampling: Science and Practice.* New York: John Wiley & Sons, 1989.
6. **Pui, D.Y.H., Y. Ye, and B.Y.H. Liu:** Experimental study of particle deposition on semiconductor wafers. *Aerosol Sci. Technol. 12(4)*:795–804 (1990).
7. **Tsai, C.-J. and D.Y.H. Pui:** Numerical study of particle deposition in bends of a circular cross-section-laminar flow regime. *Aerosol Sci. Technol. 12(4)*:813–831 (1990).
8. **Liu, B.Y.H., D.Y.H. Pui, K.L. Rubow, and W.W. Szymanski:** Electrostatic effects in aerosol sampling and filtration. *Ann. Occup. Hyg. 29(2)*:251–269 (1985).
9. **Hangal, S. and K. Willeke:** Aspiration efficiency: unified model for all forward sampling angles. *Environ. Sci. Technol. 24(5)*:688 691 (1990).
10. **Fairchild, C.I., M.I. Tillery, J.P. Smith, and F.O. Valdez:** *Collection Efficiency of Field Sampling Cassettes.* [Contract report no. LA-8640-MS] Los Alamos, New Mexico: Los Alamos National Laboratory, 1980.
11. **Speight, R.G. and A.H. Marsh:** Use of a cowl in asbestos air sampling. *Ann. Occup. Hyg. 28(3)*:353–354 (1984).
12. **Knight, K.L., D.M. Bloor, and F. Miller:** Use of a cowl in asbestos air sampling. *Ann. Occup. Hyg. 29(2)*:289–291 (1985).
13. **Tannahill, S.N., M.H. Jackson, and R.J. Willey:** Effect of cowl on air samples for amosite in the workplace and in the laboratory. *Ann. Occup. Hyg. 34(5)*:521–527 (1990).
14. **Cornett, M.J., C.H. Rice, V. Herzberg, and J. Lockey:** Assessment of fiber deposition on the conductive cowl in the refractory ceramic fiber industry. *Appl. Ind. Hyg. 4(8)*:201–204 (1989).
15. **Wang, C.C., R.A. Fletcher, E.B. Steel, and J.W. Gentry:** Measurement of the uniformity of particle deposition of filter cassette sampling in a low velocity wind tunnel. *J. Aerosol Sci. 21(suppl. 1)*:S621–S624 (1990).
16. **Baron, P.A.:** Overloading and electrostatic effects in asbestos fiber sampling. *Am. Ind. Hyg. Assoc. J. 48*:A709–A710 (1987).
17. **Johnston, A.M., A.D. Jones, and J.H. Vincent:** The effect of electrostatic charge on the aspiration efficiencies of airborne dust samplers: with special reference to asbestos. *Am. Ind. Hyg. Assoc. J. 48*: 613–621 (1987).
18. **Baron, P.A. and G.J. Deye:** Electrostatic effects in asbestos sampling I: experimental measurements. *Am. Ind. Hyg. Assoc. J. 51*:51–62 (1989).
19. **Baron, P.A. and G.J. Deye:** Electrostatic effects in asbestos sampling II: comparison of theory and experiment. *Am. Ind. Hyg. Assoc. J. 51*: 63–69 (1989).
20. **Soderholm, S.C.:** Proposed international conventions for particle size-selective sampling. *Ann. Occup. Hyg. 33(3)*:301–320 (1989).
21. **Lippmann, M.:** Asbestos exposure indices. *Environ. Res. 46*:86–106 (1988).
22. **American Conference of Governmental Industrial Hygienists:** Particle Size-Selective Sampling in the Workplace. In *Annals of the ACGIH.* Cincinnati: ACGIH, 1984. p. 23–100.
23. **Baron, P.A.:** Measurement of Asbestos and Other Fibers. In *Measurement of Aerosols: Principles, Techniques, and Applications.* K. Willeke and P.A. Baron, eds. New York: Van Nostrand Reinhold. 1993.
24. **Stöber, W., H. Flachsbart, and D. Hochrainer:** The aerodynamic diameter of latex aggregates and asbestos fibers. *Staub-Reinhalt. Luft 30(7)*:1–12 (1970).
25. **Hemenway, D.R. and S.M. MacAskill:** Design, development, and test results of a horizontal flow inhalation toxicology facility. *Am. Ind. Hyg. Assoc. J. 43*:874–879 (1982).
26. **Reischl, G., W. John, and W. Devor:** Uniform electrical charging of monodisperse aerosols. *J. Aerosol Sci. 8*:55–65 (1977).
27. **Hemenway, D.R., K. Boudreau, and J. Miller:** Retrofitting of a Wright dustfeed. *Am. Ind. Hyg. Assoc. J. 47*:301–307 (1986).
28. **Cheng, Y.S. and C.S. Wang:** Motion of particles in bends of circular pipes. *Atmos. Environ. 15*:301–306 (1981).
29. **Heyder, J. and J. Gebhart:** Gravitational deposition of particles from laminar aerosol flow through inclined circular tubes. *J. Aerosol Sci. 8*:289–295 (1977).
30. **Mark, D. and J.H. Vincent:** A new personal sampler for airborne total dust in workplaces. *Ann. Occup. Hyg. 30*:89–102 (1986).
31. **Vincent, J.H., R.J. Aitken, and D. Mark:** Further studies of porous plastic foam filtration media. *J. Aerosol Sci. 23(Suppl. 1)*: 5627–5630 (1992).